# Time-evolving genetic networks reveal a NAC troika that negatively regulates leaf senescence in *Arabidopsis*

Hyo Jung Kim[a,1], Ji-Hwan Park[a,1], Jingil Kim[a], Jung Ju Kim[a], Sunghyun Hong[a], Jeongsik Kim[a], Jin Hee Kim[a], Hye Ryun Woo[b], Changbong Hyeon[c], Pyung Ok Lim[b,2], Hong Gil Nam[a,b,2], and Daehee Hwang[a,b,2]

[a]Center for Plant Aging Research, Institute for Basic Science (IBS), Daegu 42988, Republic of Korea; [b]Department of New Biology, Daegi Gyeongbuk Institute of Science and Technology (DGIST), Daegu 42988, Republic of Korea; and [c]Korea Institute for Advanced Study, Seoul 02455, Republic of Korea

Edited by Richard Scott Poethig, University of Pennsylvania, Philadelphia, PA, and approved April 19, 2018 (received for review December 11, 2017)

**Senescence is controlled by time-evolving networks that describe the temporal transition of interactions among senescence regulators. Here, we present time-evolving networks for NAM/ATAF/CUC (NAC) transcription factors in *Arabidopsis* during leaf aging. The most evident characteristic of these time-dependent networks was a shift from positive to negative regulation among NACs at a presenescent stage. ANAC017, ANAC082, and ANAC090, referred to as a "NAC troika," govern the positive-to-negative regulatory shift. Knockout of the NAC troika accelerated senescence and the induction of other *NACs*, whereas overexpression of the NAC troika had the opposite effects. Transcriptome and molecular analyses revealed shared suppression of senescence-promoting processes by the NAC troika, including salicylic acid (SA) and reactive oxygen species (ROS) responses, but with predominant regulation of SA and ROS responses by ANAC090 and ANAC017, respectively. Our time-evolving networks provide a unique regulatory module of presenescent repressors that direct the timely induction of senescence-promoting processes at the presenescent stage of leaf aging.**

leaf senescence | time-evolving network | NAC | presenescent repressors | salicylic acid response

In plants, aging involves age-dependent developmental changes during the lifespan. At the end of aging, plants undergo senescence followed by death of cells, tissues, organs, or the entire organism. Leaf senescence is crucial for the fitness and survival of plants (1). During growth, leaves harvest solar energy and accumulate chemical energy and biomass through carbon fixation. When leaves enter senescence after a prolonged productive photosynthetic period, leaf cells undergo drastic physiological, biochemical, and metabolic changes in an orderly manner. The most obvious phenotypic change during senescence is the yellowing of leaves caused by the breakdown of chlorophyll in chloroplasts. Other metabolic changes include increased oxidation and hydrolysis of macromolecules, such as proteins, lipids, and nucleic acids. These hydrolyzed molecules in senescing leaves are recycled as materials and energy to newly developing organs or offspring in annual plants. Thus, the timely onset of leaf senescence is critical for effective recycling of materials and energy.

Leaf senescence is regulated over a long period of time in a complex manner, involving time-dependent interactions with various developmental and environmental signals (1). Genetic screens have revealed mutants with accelerated or delayed leaf senescence and thus have uncovered key regulators of leaf senescence (2–4). However, these screens are limited to the identification of one regulator per mutant rather than a regulatory module of multiple genes. Moreover, these approaches identify individual senescence regulators based on only a few phenotypes in a narrow time window of senescence, mostly at senescent stages, thus limiting insights into the regulators acting at presenescent or early stages of leaf senescence. Alternative screening approaches are needed to discover these early regulators or regulatory modules of leaf senescence.

Time-course gene-expression profiling of *Arabidopsis* leaves during aging was used recently as an alternative approach to uncover senescence regulators (5, 6). Woo et al. (5) and Breeze et al. (6) provided thousands of senescence-associated genes with differential expression during leaf aging. Potential early regulators [e.g., receptors, kinases, phosphatases, and transcription factors (TFs)] can be predicted from genes with altered expression at early stages. Moreover, regulatory modules can also be proposed as subsets of the potential early regulators. However, it is difficult to prioritize potential regulators and regulatory modules for functional validation. To resolve this issue, network analysis has often been combined with time-course gene-expression analysis. For instance, Penfold et al. (7) built a regulatory network model of senescence-regulator candidates using time-course gene-expression data (6) and prioritized key senescence regulators based on their degrees of centrality in the network model. Also, Allu et al. (8) built a coexpression network model for senescence- or stress-related

## Significance

**Leaf senescence is regulated in a complex manner, involving time-dependent interactions with developmental and environmental signals. Genetic screens have identified key regulators of senescence, particularly late-stage senescence regulators. Recently, time-course gene-expression and network analyses, mostly analyses of static networks, have predicted many senescence regulators. However, senescence is defined by time-evolving networks, involving the temporal transition of interactions among senescence regulators. Here, we present time-evolving networks of NAM/ATAF/CUC (NAC) transcription factors, central regulators of leaf senescence in *Arabidopsis*, via time-course gene-expression analysis of NACs in their mutants. These time-evolving networks revealed a unique regulatory module of NACs that controls the timely induction of senescence-promoting processes at a presenescent stage of leaf aging.**

Author contributions: H.J.K., H.R.W., P.O.L., H.G.N., and D.H. designed research; H.J.K., J.-H.P., J.G.K., J.J.K., S.H., J.K., and J.H.K. performed research; H.J.K., J.-H.P., J.G.K., J.J.K., S.H., J.K., J.H.K., H.R.W., C.H., P.O.L., H.G.N., and D.H. analyzed data; and H.J.K., J.-H.P., P.O.L., H.G.N., and D.H. wrote the paper.

The authors declare no conflict of interest.

This article is a PNAS Direct Submission.

This open access article is distributed under Creative Commons Attribution-NonCommercial-NoDerivatives License 4.0 (CC BY-NC-ND).

Data deposition: The raw and normalized data of the Nanostring nCounter assay and RNA sequencing have been deposited in the National Center for Biotechnology Information Gene Expression Omnibus database (accession nos. GSE92369 and GSE92314, respectively) under the GEO SuperSeries accession no. GSE92371.

[1]H.J.K. and J.-H.P. contributed equally to this work.

[2]To whom correspondence may be addressed. Email: polim@dgist.ac.kr, nam@dgist.ac.kr, or dhwang@dgist.ac.kr.

This article contains supporting information online at www.pnas.org/lookup/suppl/doi:10.1073/pnas.1721523115/-/DCSupplemental.

Published online May 7, 2018.

genes (salt and oxidative stress) and predicted a regulatory module as a set of densely interacting nodes in the network model. In these approaches, network models delineate static views of interactions among candidate senescence regulators. However, senescence is determined by time-dependent interactions among senescence regulators during leaf aging. Thus, there is a need for a method based on time-evolving networks that describe the temporal transition of regulatory interactions among senescence regulators during leaf aging.

Several types of senescence regulators have been reported in plants, including receptors, kinases/phosphatases, TFs, epigenetic regulators (e.g., methyltransferases and demethylases), and regulatory RNAs (e.g., microRNAs) (3). Of these, the TFs, such as NACs (NAM/ATAF/CUC), WRKYs, and MYBs, are important for regulating the temporal expression of senescence-associated genes during leaf aging (3, 9–16). Among the TF families, the NAC family is one of the largest (17, 18) and is a central regulator of leaf senescence. Many NACs (57.5% or 65/113 NAC genes) show expression changes during leaf aging in *Arabidopsis*, and genetic studies identified many NACs as positive (ANAC016, ANAC029/AtNAP, ANAC059/ORS1, and ANAC092/ORE1) and negative (ANAC042/JUB1 and ANAC083/VNI2) regulators of leaf senescence (4, 19–24). Moreover, the NACs are reported to regulate their own and each other's transcription (25). Thus, time-evolving regulatory networks for NACs likely provide sufficient information regarding the temporal transition of regulatory relationships, thereby enabling the prioritization of NACs or NAC-regulatory modules involved in leaf senescence.

Here, we present time-evolving networks that delineate causal regulatory relationships among 49 senescence-associated NACs, revealing a shift from positive to negative regulation among NACs before senescence. Three NACs, ANAC017, ANAC082, and ANAC090, referred to as a "NAC troika" (regulatory module), governed this regulatory shift. We found that the NAC troika negatively regulates leaf senescence at presenescent stages by inhibiting senescence-promoting pathways, including salicylic acid (SA) and reactive oxygen species (ROS) pathways.

## Results

**Time-Evolving NAC Networks Reveal a Regulatory Shift at a Presenescent Stage.** In our network-based approach, we first selected a set of senescence regulators to construct time-evolving networks. Among 113 *NAC*s in *Arabidopsis* (26), we selected the 65 *NAC*s that show gene-expression changes over the lifespan of leaves (*SI Appendix*, Fig. S1*A*) (5). To infer the temporal evolution of regulatory relationships among the selected NACs, we obtained knockout mutants for 49 of the 65 *NAC*s from the Arabidopsis Biological Resource Center (*SI Appendix*, Table S1). We sampled the third and fourth true leaves of wild-type (Col) and mutant plants at 4-d intervals from a mature leaf stage (14 d of leaf age) to a middle-senescent stage (26 d of leaf age) that displays more than 40% loss of chlorophyll (*SI Appendix*, Fig. S1 *B–E*). Previously, transcript levels of *SEN4*, a senescence-inducible marker, were reported to be significantly (twofold or more) increased in leaves at 22 d of leaf age, compared with those at the mature stage (14 d), with about a 20% loss of chlorophyll (27). We thus defined 22 d of leaf age as an early senescent stage and 18 d of leaf age, between the mature (14 d) and early-senescent (22 d) stages, as a presenescent stage.

We measured mRNA-expression levels in wild-type and mutant leaves at these four stages (mature and pre-, early-, and middle-senescent stages) by NanoString nCounter analysis (28). For each stage, we identified differentially expressed *NAC*s in individual mutants relative to the wild type, which were considered targets of the mutated *NAC*. Up- and down-regulation of the target *NAC*s in mutants reflect negative (repressive) and positive (activating) regulation, respectively, in wild-type plants (Fig. 1*A*). In total, 148, 140, 120, and 91 differentially expressed *NAC*s were identified from the 49 *NAC* mutants at 14, 18, 22, and 26 d of leaf age, respectively (Dataset S1). For each stage, we built a genetic regulatory network that describes positive and negative regulatory relationships between the mutated *NAC*s and their target *NAC*s (Fig. 1*B*).

Intriguingly, the time-evolving NAC networks revealed a drastic inversion in the dominant regulatory patterns from positive regulation at 14 d (mature stage) to negative regulation at 18 d (presenescent stage) (Fig. 1*B*). The number of positive regulations decreased from 86 at 14 d to 10 at 18 d (8.6-fold), whereas the number of negative regulations increased from 62 to 130 (2.1-fold) (Fig. 1*C*). Negative regulations remained dominant after 18 d (Fig. 1*C* and *SI Appendix*, Fig. S1 *F* and *G*). The positive-to-negative regulatory inversion in the time-evolving NAC networks suggests the suppression or maintenance of *NAC* expression, possibly as a strategy to prevent untimely senescence at the presenescent stage.

We next attempted to identify early-senescence regulators or regulatory modules from the time-evolving network. Many biological networks have been shown to be scale-free with the hubs that govern functions of the networks (29). Our NAC networks were also found to be scale-free at individual stages based on out-degree distributions (29), suggesting the presence of hub NACs at individual stages (*SI Appendix*, Fig. S2*A*). This observation led us to hypothesize that such hub NACs can govern the positive-to-negative regulatory inversion at the presenescent stage. To test this hypothesis, we identified seven hub NACs that have a significantly ($P < 1.0 \times 10^{-4}$) large number of target *NAC*s (i.e., significant out-degree centrality) in the time-evolving networks, as described in *SI Appendix*, *SI Materials and Methods* [*SI Appendix*, Fig. S2*B*: ANAC083 at 14 d (mature); ANAC017, ANAC082, and ANAC090 at 18 d (presenescent); ANAC055 and ANAC090 at 22 d (early senescent); and ANAC076 and ANAC079 at 26 d (middle senescent)]. The subnetworks for the hub NACs and their targets showed that the hub NAC at 14 d (ANAC083) regulated its targets positively and negatively, whereas the hub NACs from 18 to 26 d regulated their targets only negatively (Fig. 1*D*), indicating the importance of the hub NACs at 18 d in the establishment of the regulatory inversion. To further assess such importance, we evaluated whether removing the hub NACs from the time-evolving networks affected the positive-to-negative regulatory inversion. Among the hub NACs, the three hub NACs ANAC017, ANAC082, and ANAC090 at 18 d, as a NAC troika, showed the most significant reduction ($P < 1.0\times10^{-4}$) in negative regulations, suggesting that the NAC troika has the largest effect on the regulatory inversion (Fig. 1*E*).

We confirmed target *NAC*s of the NAC troika at 18 d by quantitative real-time PCR (qRT-PCR) (Fig. 1*F*). Finally, we examined whether the perturbation of the NAC troika could affect the induction kinetics of their target *NAC*s at the presenescent stage. The induction of target *NAC*s was accelerated in single and double mutants of the NAC troika compared with wild-type plants, whereas plants overexpressing the NAC troika displayed delayed the induction of target *NAC*s (*SI Appendix*, Fig. S3), suggesting that the NAC troika critically contributes to the regulatory inversion kinetics in time-evolving NAC networks. Taken together, these data suggest that the NAC troika, as a regulatory module of early-senescence regulators, controls the positive-to-negative regulatory inversion at the presenescent stage in the time-evolving NAC networks.

**The NAC Troika Negatively Regulates Various Leaf-Senescence Phenotypes.** Next, we investigated the physiological relevance of the presenescent regulatory inversion in the time-evolving NAC networks. To this end, we examined whether the NAC troika that governs this inversion was associated with leaf senescence. First, we measured two physiological features of leaf senescence, chlorophyll content and photochemical efficiency (Fv/Fm), in the mutants of the seven hub *NAC*s during leaf aging. Consistent with

PLANT BIOLOGY

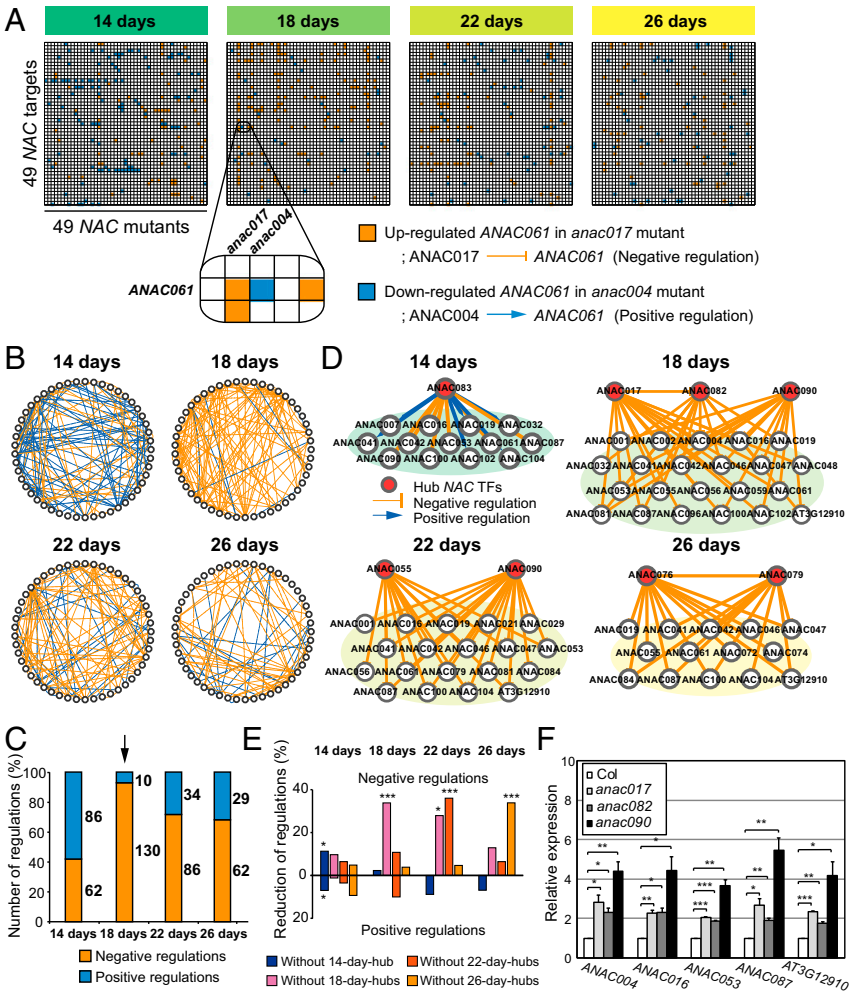


**Fig. 1.** Time-evolving NAC networks reveal a drastic inversion in their regulatory patterns at the presenescent stage. (*A*) Causal regulatory relationships among 49 aging-associated *NAC*s at four stages (14, 18, 22, and 26 d of leaf age). The heat map at each stage shows the relationships inferred from differentially expressed *NAC*s between *NAC*-knockout mutants and wild-type plants at 14, 18, 22, and 26 d. For example, *ANAC061* was up-regulated (orange in the heat map) in the *anac017* mutant, indicating negative (repressive) regulation on *ANAC061* by ANAC017. In contrast, *ANAC061* was down-regulated (blue in the heat map) in the *anac004* mutant, indicating positive (activating) regulation on *ANAC061* by ANAC004. (*B*) Genetic regulatory networks that show causal regulatory relationships among 49 *NAC*s at the four stages. In each network, circles represent 49 NACs, and the blue and orange lines indicate positive and negative regulations inferred from *NAC*s differentially expressed in the mutants and the wild type. (*C*) Relative proportions of positive (blue) and negative (orange) regulations at each stage. The arrow indicates the presenescent stage (18 d) in which the number of negative regulations exceeded that of positive regulations, referred to as the "positive-to-negative regulatory inversion." (*D*) Subnetworks showing negative (orange) and positive (blue) regulatory relationships between hub NACs and their target *NAC*s at four stages (14, 18, 22, and 26 d of leaf age). In each subnetwork, circles represent target *NAC*s regulated by the corresponding hub NACs, and blue and orange lines indicate positive and negative regulations of target *NAC*s by the hub NACs. (*E*) Reduced percentages of negative and positive regulatory relationships at each stage after removing the hub NACs identified at individual stages from the time-evolving networks. Colors represent the percentages after removal of the indicated hub NACs. The significance (*P*) of the reduction percentage was evaluated using an empirical distribution of the reduction percentage obtained from random removal experiments. $^{*}P < 0.05$; $^{***}P < 0.001$. (*F*) Validation of the up-regulation of five representative *NAC* targets in *anac017*, *anac082*, and *anac090* mutants at 18 d. mRNA expression levels were analyzed by qRT-PCR and then were normalized by those of *ACT2*. For each gene, the normalized expression levels were further normalized by those in wild-type plants. The normalized expression levels were compared with those in wild-type plants using ANOVA with Dunnett's correction as a post hoc test. $^{*}P < 0.1$; $^{**}P < 0.05$; $^{***}P < 0.01$. Values are means ± SE ($n = 3$).

the findings in Fig. 1*E*, among the seven identified hub NACs, the mutants of the NAC troika showed the most substantial acceleration in the loss of chlorophyll content and photochemical efficiency compared with the wild type (Fig. 2 *A* and *B* and *SI Appendix*, Fig. S4).

Next, we examined the role of the NAC troika in leaf-yellowing phenotypes, cell death, and the expression of molecular senescence markers during leaf aging. The overall growth and development of *anac017*, *anac082*, and *anac090* mutants were not significantly distinguishable from those of wild-type plants (Fig. 2*C*). However, rosette leaves (the third or fourth leaf) of *anac017*, *anac082*, and *anac090* mutants began to yellow at 30 d of leaf age and were completely yellow at 34 d, whereas wild-type leaves retained their integrity and remained green even at 34 d (Fig. 2*D*). In addition, Trypan blue staining revealed increased cell death in the third or fourth leaves of *anac017*, *anac082*, and *anac090* mutants relative to the wild type (Fig. 2*E*). Consistent with these findings, these mutants exhibited accelerated induction of two senescence marker genes, *SEN4* and *SAG12*, during leaf aging, compared with the wild type (Fig. 2 *F* and *G*). Further, double mutants of the NAC troika exhibited accelerated leaf yellowing compared with the single mutants, whereas overexpression plants

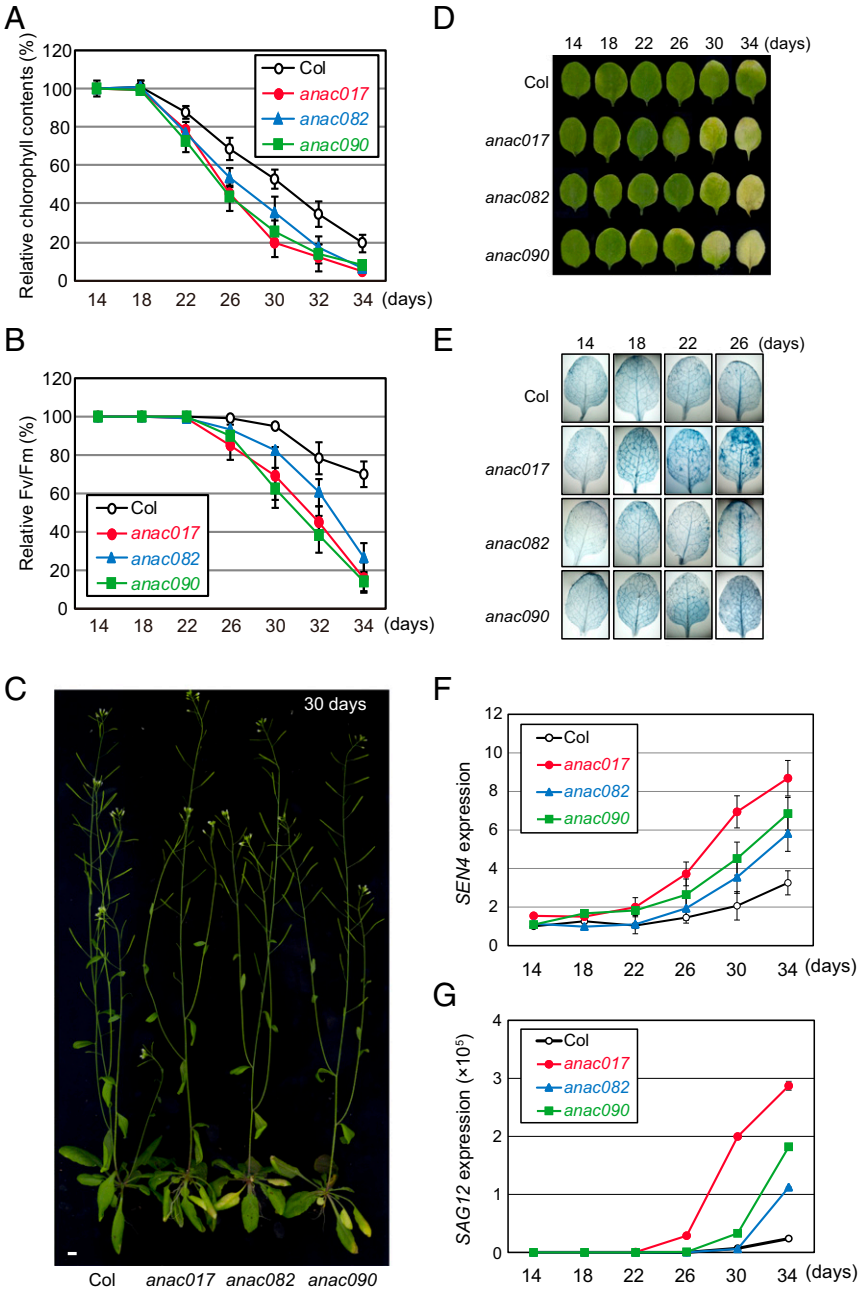


**Fig. 2.** Mutants of the NAC troika exhibit strong associations with leaf-senescence phenotypes. (*A* and *B*) Relative changes in chlorophyll content (*A*) and photochemical efficiency (Fv/Fm) (*B*) in single mutants of the NAC troika (*anac017*, *anac082*, and *anac090* mutants) compared with wild-type (Col) plants during leaf aging. Values are means ± SD ($n > 20$) and are normalized to those at 14 d in individual mutants. Colors represent the data measured from the indicated single mutants. (*C*) Representative photographs of a wild-type plant (Col) and single mutants at 30 d after the emergence of the third or fourth leaves. (Scale bar, 1 cm.) (*D*) Leaf yellowing in wild-type plants and single mutants at the indicated leaf age (in days). (*E*) Trypan blue staining of leaves at the indicated leaf age. In each plant, blue-colored patches of cells were developed by Trypan blue staining, indicating areas of dead or dying cells. (*F* and *G*) mRNA expression levels of *SEN4* (*F*) and *SAG12* (*G*) in wild-type plants and single mutants at the indicated leaf age. The mRNA expression level of each gene was measured by qRT-PCR and normalized by that of *ACT2*. Values are means ± SD ($n = 2$).

showed delayed leaf yellowing (*SI Appendix*, Fig. S5*A*). Similar patterns were observed for chlorophyll loss (*SI Appendix*, Fig. S5*B*), which was measured as the median relative chlorophyll content during leaf aging, and for the expression of *SAG12* (*SI Appendix*, Fig. S5*C*). Taken together, these data show that the NAC troika is strongly associated with leaf senescence, suggesting that the presenescent regulatory shift governed by the NAC troika in the time-evolving NAC networks is linked to leaf senescence.

**The NAC Troika Suppresses Genes Involved in Senescence-Promoting Processes.** To investigate senescence-associated genes regulated by the NAC troika, we performed genome-wide mRNA expression analysis of wild-type and mutant leaves at the presenescent stage (18 d) (Fig. 3*A*). We compared the transcriptomes of wild-type leaves with those of *anac017*, *anac082*, and *anac090* mutants and identified 1,977, 1,355, and 1,907 differentially expressed genes (DEGs), respectively (Dataset S2) (30). We found that 1,796 (72.6%) of the union of these DEGs (2,473 genes) were differentially

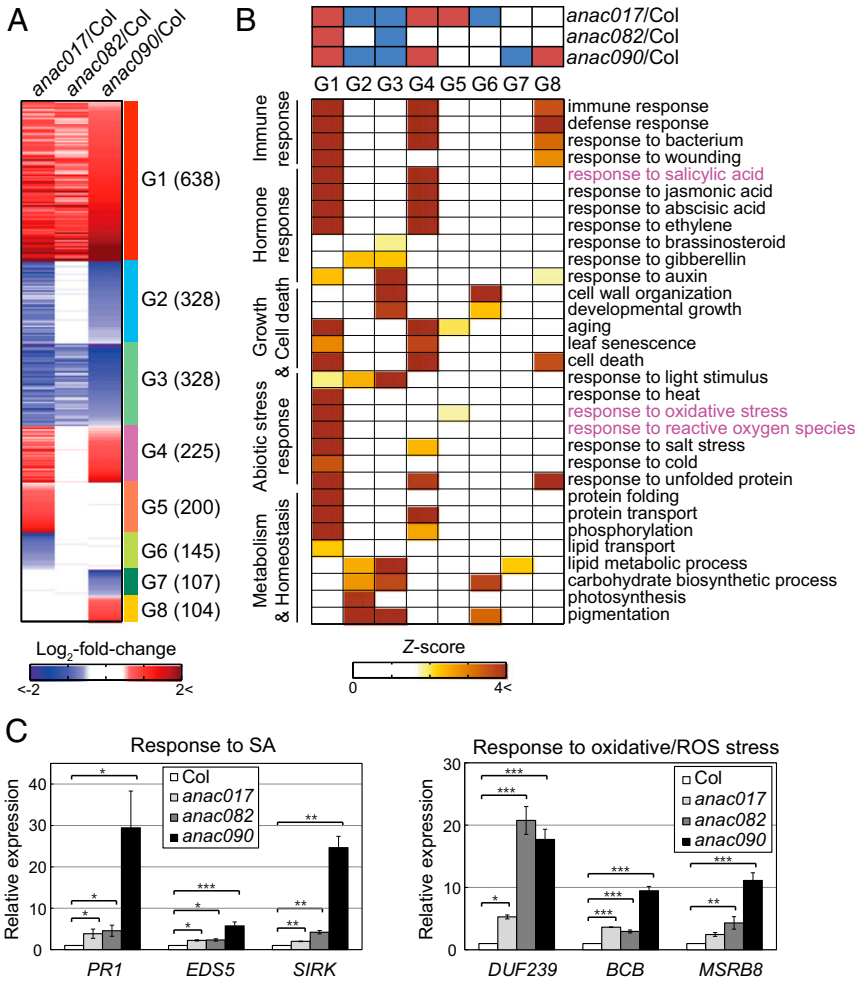


**Fig. 3.** The NAC troika negatively regulates genes involved in senescence-promoting processes. (*A*) Heat map showing eight major groups (G1–8) of genes up-regulated (red) and down-regulated (blue) in *anac017*, *anac082*, and *anac090* mutants compared with the wild type. The numbers of target genes in each group are denoted in parentheses. Red and blue colors represent up- and down-regulation in the mutants, respectively, compared with the wild type. The color bar shows the gradient of $\log_2$ fold changes between the mutants and the wild type. (*B*) GOBPs represented by the genes in G1–8. (*Upper*) The heat map shows up-regulation (red) and down-regulation (blue) patterns of the genes in G1–8 from the three comparisons: *anac017* vs. wild type (*anac017*/Col), *anac082* vs. wild type (*anac082*/Col), and *anac090* vs. wild type (*anac090*/Col). (*Lower*) The heat map shows the significance (*Z*-score) of GOBPs being enriched by the genes in G1–8. The enriched GOBPs were categorized into the following functional groups: immune response, hormone response, growth and cell death, abiotic stress response, and metabolism and homeostasis. Two top-ranked GOBPs according to GOBP-association analysis (*SI Appendix*, Fig. S5 *B* and *C*), responses to SA, and oxidative/ROS stress, are labeled in magenta. The color bar shows the *Z*-score gradient that represents the enrichment significance (*P* value): $Z = N^{-1}(1 - P)$ where $N^{-1}$ is the inverse standard normal distribution and *P* is the enrichment *P* value. (*C*) Confirmation of up-regulation of SA- and oxidative/ROS stress-inducible genes in the mutants, compared with wild-type plants, at 18 d using qRT-PCR analysis. mRNA expression levels of SA-inducible genes (*PR1*, *EDS5*, and *SIRK*) and oxidative/ROS stress-inducible genes (*DUF239*, *BCB*, and *MSRB8*) were measured by qRT-PCR and then were normalized by those of *ACT2*. For each gene, the normalized expression level was further normalized by that in wild-type plants. The normalized expression levels were compared with those in wild-type plants using one-way ANOVA with Dunnett's correction as a post hoc test. $^*P < 0.05$; $^{**}P < 0.01$; $^{***}P < 0.001$. Values are means ± SE ($n$ = 3 or 4).

expressed in more than one mutant (*SI Appendix*, Fig. S6*A*), suggesting substantial coregulation by the NAC troika.

We categorized the 2,473 DEGs into 21 groups based on their patterns of up- and down-regulation in the three mutants relative to the wild type (*SI Appendix*, Table S2). We focused on eight major groups (G1–8), each of which includes more than 100 DEGs (Fig. 3*A*). To determine the cellular processes associated with the genes in G1–8, we performed enrichment analysis of Gene Ontology (GO) biological processes (GOBPs) (Dataset S3) (31). Groups G1 and G4 were significantly ($P < 0.01$) associated with aging and leaf senescence (Fig. 3*B*); groups G2 and G3 were mainly associated with developmental growth (photosynthesis and carbohydrate/lipid metabolism) and responses to development and growth hormones (brassinosteroid and gibberellin); and groups G5–8 were associated with subsets of these processes. Based on these results, we focused on groups G1 and G4 that were significantly associated with aging and leaf senescence (Fig. 3*B*). Moreover, G1 was more strongly associated than G4 with senescence-promoting processes such as immune responses, responses to abiotic stresses (oxidative/ROS and salt stresses), and responses to senescence-promoting hormones [SA, jasmonic acid (JA), abscisic acid (ABA), and ethylene]. Furthermore, among these processes, the GOBP-association analysis revealed that responses to SA and oxidative/ROS stress are the top senescence-promoting processes regulated by the NAC troika (*SI Appendix*, Fig. S6 *B* and *C*). Finally, using qRT-PCR analysis, we confirmed that genes involved in responses to SA (*PR1*, *EDS5*, and *SIRK*) and ROS (*DUF239*, *BCB*, and *MSRB8*) were up-regulated in

presenescent-stage leaves from the mutants compared with the wild type (Fig. 3*C*). Collectively, these data suggest that the NAC troika negatively regulates senescence-promoting processes, including responses to SA and oxidative/ROS stress, at the presenescent stage.

**ANAC090 and ANAC017 Predominantly Suppress SA and ROS Responses, Respectively, at the Presenescent Stage.** Next, to identify genes that are differentially regulated by each component of the NAC troika, we compared expression profiles among single mutants. We identified 221 genes that were up-regulated in *anac017* relative to *anac082* and *anac090* (P1), 129 genes that were up-regulated in *anac082* relative to *anac017* and *anac90* (P2), and 172 genes that were up-regulated in *anac90* relative to *anac017* and *anac082* (P3) (Fig. 4*A*). Similarly, we identified 87, 149, and 118 genes that were specifically down-regulated in *anac017*, *anac082*, and *anac090* mutants, respectively, compared with the other single mutants (P4–6 in Fig. 4*A*; also see *SI Appendix*, *SI Materials and Methods* and Dataset S4). GOBP enrichment analysis for the genes in P1–6 revealed that responses to SA and oxidative/ROS stress were more strongly represented by the up-regulated genes in *anac090* (P3) and *anac017* (P1) mutants, respectively (Fig. 4*B* and Dataset S5). Consistently, ANAC017 was reported to regulate more than 80% of genes involved in the response to hydrogen peroxide ($H_2O_2$) in *Arabidopsis*, thereby conferring the hypersensitivity to $H_2O_2$ in *anac017* mutants (32). However, little is known about SA-associated functions of ANAC090 in leaf senescence. To further investigate this differential regulation of the SA response by ANAC090, we measured endogenous steady-state levels of SA in the leaves of wild-type plants and in single and double mutants at 18 d of leaf age. Total and free SA levels were elevated in leaves with an *anac090* mutation (*anac090*, *anac017/090*, and *anac082/090*) relative to those without this mutation (Fig. 4*C*), suggesting a predominant role for ANAC090 in suppressing SA accumulation at the presenescent stage.

Next, to investigate the differential regulation of the ROS response by ANAC017, we measured ROS, superoxide ($O_2^-$), and $H_2O_2$ content in leaves from wild-type plants and single and double mutants at 18 d of leaf age. $O_2^-$ and $H_2O_2$ levels were much higher in leaves containing an *anac017* mutation (*anac017* and *anac017/082* mutants) than in those without this mutation (Fig. 4*D*), suggesting a prominent role for ANAC017 in regulating ROS levels at the presenescent stage. Interestingly, despite the presence of an *anac017* mutation, $O_2^-$ and $H_2O_2$ levels in the *anac017/090* mutant did not differ from wild-type levels, suggesting potential crosstalk between *anac017* and *anac090* on the regulation of oxidative stress (*Discussion*). Consistent with these observations, the mRNA levels of *PR1*, a marker of SA induction, were increased significantly ($P < 0.01$) in *anac090*, *anac017/090*, and *anac082/090* mutants (Fig. 4*E*), whereas the mRNA levels of *At2g21640*, previously reported as a marker of oxidative stress (33), were significantly ($P < 0.001$) increased in *anac017* and *anac017/082* mutants but not in *anac017/090* mutants (Fig. 4*F*). On the other hand, the GOBP enrichment analysis above showed the shared regulation of SA and ROS responses by the NAC troika (Fig. 3*B*), suggesting that a subset of genes or additional genes involved in SA and ROS responses were more strongly regulated by ANAC090 and ANAC017, respectively (P3 and P1, respectively, in Fig. 4*A*) (*Discussion*). Taken together, these results suggest that the NAC troika collectively suppresses the induction of genes involved in senescence-promoting processes (Fig. 3*B*) but with additional predominant regulation of genes involved in SA and ROS responses by ANAC090 and ANAC017, respectively (Fig. 4*G*).

**ANAC090 Directly Binds and Suppresses Promoters of Target Genes Involved in the SA Response.** Having established that the NAC troika influences leaf-senescence phenotypes via negative regulation of target genes that promote senescence, we next examined whether the NAC troika binds directly to promoters of their target genes. We generated plants overexpressing GFP-tagged ANAC090 (*SI Appendix*, Fig. S7 *A* and *B*) and performed ChIP-PCR for SA-inducible genes (*PR1*, *EDS5*, and *SIRK*) (Fig. 3*C*) and for *ICS1*, a key SA synthetic enzyme gene. We found that ANAC090 bound to the promoters of all tested SA-inducible genes (Fig. 5*A* and *SI Appendix*, Fig. S7*C*) as well as to the promoters of the previously tested seven target *NAC*s of the NAC troika (*ANAC0042*, *ANAC046*, *ANAC047*, *ANAC053*, *ANAC081*, *ANAC087*, and *AT3G12910*) (Fig. 5*B* and *SI Appendix*, Fig. S7*C*). Furthermore, we measured luciferase activities in protoplasts cotransfected with a *proPR1:LUC* reporter and *ANAC090-HA* and observed decreased activity of *PR1* promoter, indicating negative regulation of the *PR1* gene by ANAC090 (Fig. 5*C*). These data suggest that ANAC090 directly suppresses the expression of target genes, including *PR1*. We were unable to perform ChIP-PCR experiments with ANAC017 and ANAC082 due to the instability of these proteins after protein extraction.

NAC TFs have been shown to form homodimers or heterodimers that bind the promoters of target genes (34, 35). To determine whether the components of the NAC troika interact, we performed bimolecular fluorescence complementation (BiFC) experiments. BiFC signals were detected in the nucleus (puncta in images) for all pairwise combinations of ANAC017, ANAC082, and ANAC090 (Fig. 5*D*), revealing that they form homodimers and heterodimers. We performed coimmunoprecipitation experiments and confirmed the formation of homodimers of ANAC017 and ANAC082 (Fig. 5*E*, *Left* and *Middle*, respectively), as well as homodimers of ANAC090 and heterodimers of ANAC090 with ANAC017 and ANAC082 in protoplasts (Fig. 5*E*, *Right*). Collectively, our results suggest that the components of the NAC troika interact and directly regulate the promoters of target genes, which may contribute to the positive-to-negative regulatory inversion and/or to the inhibition of senescence-promoting processes before leaf senescence.

## Discussion

We show that the NAC troika, consisting of ANAC017, ANAC082, and ANAC090, is a negative regulator of leaf senescence that increases in mRNA expression as leaves approach senescence (*SI Appendix*, Fig. S8*A*) (5). Our findings suggest that senescence-promoting genes as well as anti-senescence regulators are up-regulated during leaf senescence, possibly to control the initiation and progression of leaf senescence. The mRNA levels of all three *NAC*s began to increase at the presenescent stage, which might underlie the positive-to-negative regulatory shift at the presenescent stage.

We showed shared regulation of SA and ROS responses by the NAC troika (Fig. 3) but also observed differential regulation of SA and ROS responses by ANAC090 and ANAC017, respectively (Fig. 4). To clarify shared and differential regulation of the NAC troika on SA and ROS responses, we built a network model that describes the interactions among the genes involved in the shared (G1 and G4 in Fig. 3*A*) and differential (P1 and P3 in Fig. 4*A*) regulation of SA and ROS responses by the NAC troika (*SI Appendix*, Fig. S8*B* and Dataset S6). For the SA response, the network model showed that the genes involved in SA synthesis (*ICS1*, *EDS5*, *CBP60G*, *SARD1*, and *MES9*) and downstream TFs of SA signaling (*MYB2*, *MYB50*, *MYB51*, *WRKY18*, *WRKY30*, *WRKY38*, *WRKY40*, *WRKY53*, *WRKY54*, *WRKY60*, *WRKY62*, *WRKY70*, and *ANAC081*) belonged to G1 or G4, suggesting that these central processes in SA response are commonly regulated by the NAC troika. However, a significant portion of these genes (*CBP60G* for SA synthesis and *WRKY18*, *WRKY38*, *WRKY40*, *WRKY53*, *WRKY54*, and *WRKY70* for SA signaling) belonged to P3, suggesting that the central processes in SA response were more strongly regulated by ANAC090 beyond their basal shared regulations with ANAC017 and ANAC082. Similarly, the network

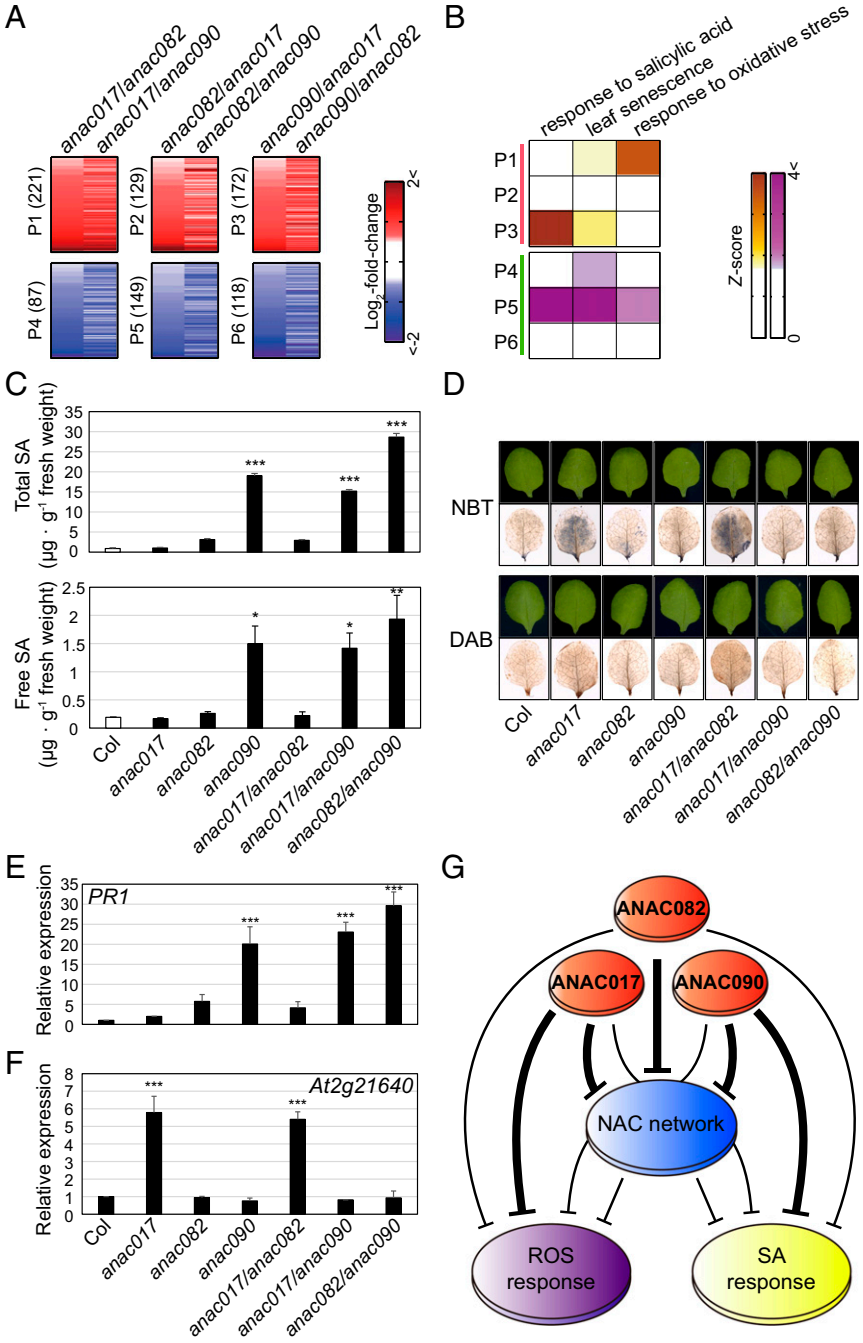


**Fig. 4.** ANAC017 and ANAC090 differentially regulate ROS and SA responses. (*A*) Heat maps showing up-regulation (red) and down-regulation (blue) of genes predominantly in *anac017* (P1 and P4), *anac082* (P2 and P5), or *anac090* (P3 and P6) mutants. These genes were identified from the following comparisons: for P1 and P4, *anac017* vs. *anac082* (*anac017/anac082*) and *anac017* vs. *anac090* (*anac017/anac090*); for P2 and P5, *anac082* vs. *anac017* (*anac082/anac017*) and *anac082* vs. *anac090* (*anac082/anac090*); and for P3 and P6, *anac090* vs. *anac017* (*anac090/anac017*) and *anac090* vs. *anac082* (*anac090/anac082*). The number of genes in each pattern is denoted in parenthesis. The color bar represents the gradient of $\log_2$ fold changes from each comparison. (*B*) Representative aging-associated GOBPs enriched by genes in P1–6. The color bar represents the *Z*-score gradient representing enrichment significance (*P* value): $Z = N^{-1}(1 - P)$ where $N^{-1}$ is the inverse standard normal distribution and *P* is the enrichment *P* value. (*C*) Endogenous levels of free SA and total SA (free SA + SA glucosides) measured from the third or fourth leaves of wild-type (Col) plants, single mutants, and double mutants at 18 d of leaf age. Values are means ± SE ($n = 3$). (*D*) Staining of $O_2^-$ and $H_2O_2$ in the third or fourth leaves of wild-type plants, single mutants, and double mutants at 18 d of leaf age using nitroblue tetrazolium (NBT) and diaminobenzidine tetrahydrochloride (DAB), respectively. (*E* and *F*) mRNA expression levels of *PR1* (*E*) and *At2g21640* (*F*) in leaves from wild-type (Col) plants, single mutants, and double mutants at 18 d of leaf age. mRNA expression levels were analyzed by qRT-PCR and then were normalized by those of *ACT2*. For each gene, the normalized expression levels were further normalized by those in wild-type plants. Values are means ± SD ($n = 4$). (*G*) A proposed model for shared and differential regulation by the NAC troika of SA and ROS responses. SA levels and the normalized expression levels were compared using one-way ANOVA with Dunnett's correction as a post hoc test. $^*P < 0.05$; $^{**}P < 0.01$; $^{***}P < 0.001$.

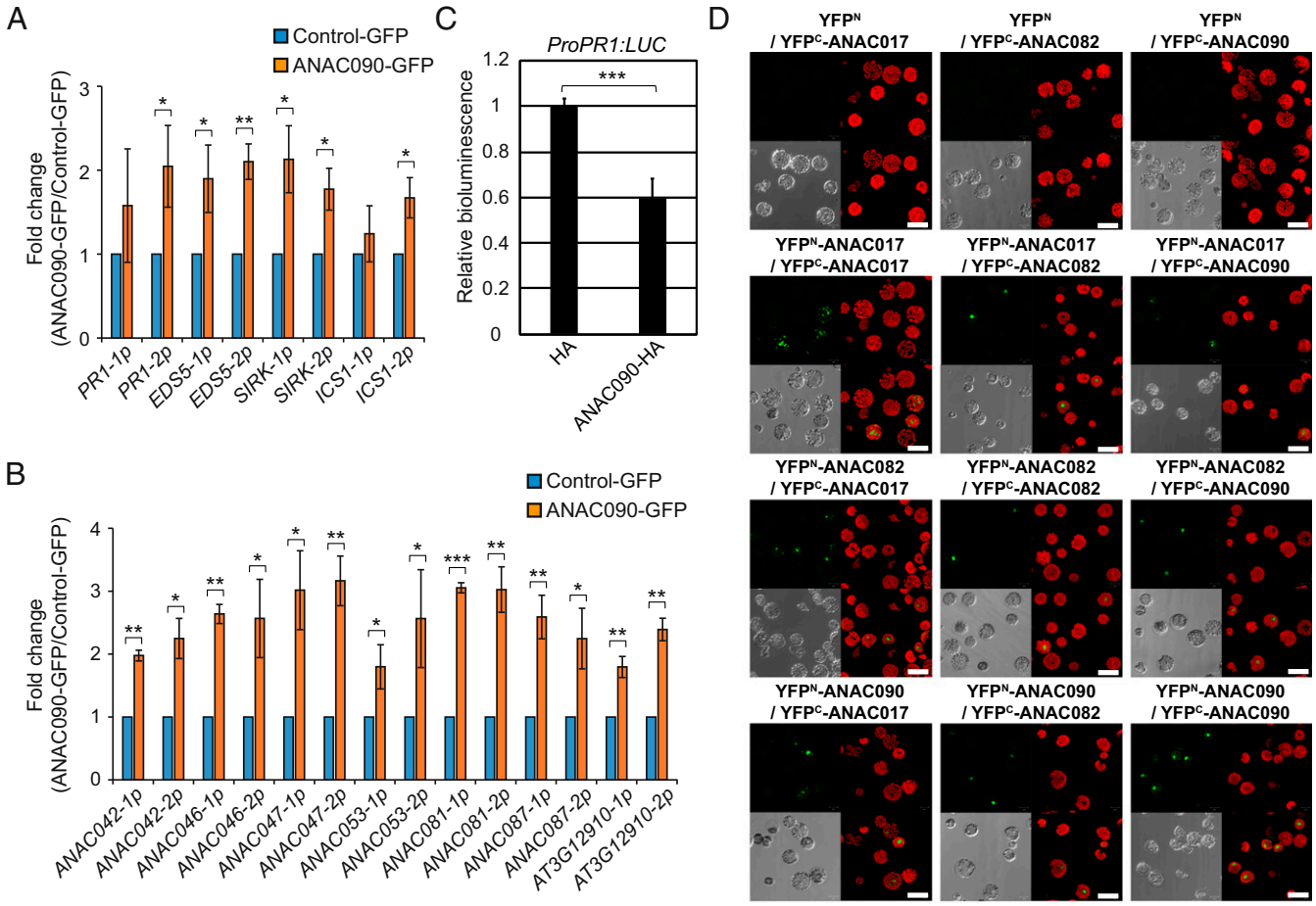


**Fig. 5.** Components of the NAC troika interact among themselves, and ANAC090 binds to the promoter of SA-inducible genes and target *NACs*. (*A* and *B*) ChIP-qPCR assays of selected DNA fragments in the promoters of SA-inducible genes (*PR1*, *EDS5*, *SIRK*, and *ICS1*) (*A*) and in the promoters of downstream target *NACs* (*ANAC042*, *ANAC046*, *ANAC047*, ANAC053, *ANAC081*, *ANAC087*, and *At3g12910*) (*B*). Chromatin from aerial parts of 2-wk-old *pCsVMV:ANAC090-GFP* plants was immunoprecipitated with an anti-GFP antibody. Enrichment fold changes were normalized to those of *TA3*. Values are means ± SD ($n = 3$). The normalized enrichment fold changes were compared between control-GFP and ANAC090-GFP samples using the paired *t* test (right-sided). $^{*}P < 0.05$; $^{**}P < 0.01$; $^{***}P < 0.001$. (*C*) Transient expression assays in *Arabidopsis* protoplasts showing the transrepression of the *PR1* promoter by ANAC090. Protoplasts were cotransfected with the *proPR1:LUC* reporter and an effector plasmid expressing ANAC090-HA. The expression of *proPR1:LUC* was normalized to that of *35Spro:RLuc* (internal control). The resulting expression in ANAC090-HA was normalized to that in protoplasts that were transfected with the reporter plasmid and an effector plasmid expressing HA only. Values are means ± SD ($n = 3$). The relative expression levels in ANAC090-HA and HA samples were compared using a *t* test. $^{***}P < 0.001$. (*D*) BiFC analysis of protein interactions among ANAC017, ANAC082, and ANAC090. Fluorescence was detected using a confocal laser-scanning microscope: BiFC fluorescence (green signal, *Upper Left*), chlorophyll fluorescence (red signal, *Upper Right*), bright-field images (*Lower Left*), and merged images (*Lower Right*) are shown. (Scale bars, 50 μm.) (*E*) Coimmunoprecipitation analysis of interactions among ANAC017, ANAC082, and ANAC090. Protoplast cells were cotransfected with the indicated combinations of HA- and GFP-tagged proteins (ANAC017, ANAC082, or ANAC090) along with the GFP control. GFP-tagged proteins and GFP control proteins were immunoprecipitated with an anti-GFP antibody (α-GFP), and the immunoblots were probed with anti-HA (α-HA) and anti-GFP antibodies.

model showed that the genes involved in ROS production (*PER34* and *PER71*) and reduction (*PER4*, *PER52*, *DUF239*, *GRXC9*, *GRXS13*, *MSRB8*, *MSRB9*, *AOX1D*, and *ANAC042*), downstream processes of ROS signaling (*CRT1* and *CRT2* for mitochondrial dysfunction and *PLP2*, *GSTF6*, *CYP71A12*, *CYP71A13*, *CYP71B15*, and *PAD4* for defense response), and NAD/NAD(P)H, FAD/$FADH_2$ regulation (*NUDT7*, *AT1G30720*, and *AT5G48440*) belonged to G1 or G4, but additional genes [*PER71* for ROS production, *PER52* for ROS reduction, *DOX1*, *CYP71A12*, *CYP79B3*, and *PAD4* for defense response, *ANAC013* for mitochondrial retrograde signaling, and *AT1G30720*, *AT5G01670*, *AT5G16980*, *AT5G44380*, and *AT5G48440* for NAD(P)/NAD(P)H and FAD/$FADH_2$ regulation] involved in the same processes belonged to P1, suggesting the basal shared regulation of ROS response and its additional regulation by ANAC017. Thus, the network model can explain how the NAC troika can commonly and differentially regulate SA and ROS responses.

In this study, we found that $O_2^-$ and $H_2O_2$ levels in *anac017/090* mutants, unlike *anac017* and *anac017/082* mutants, did not differ from wild-type levels (Fig. 4*D*). Similar to *anac017/090* mutants, *anac090* mutants showed no significant difference in the levels of $O_2^-$ and $H_2O_2$ from the wild type. On the other hand, all mutants containing the *anac090* mutation showed increased levels of SA in leaves. Previously, SA was shown to reduce ROS through the antioxidant defense system, although SA was also shown to contribute to the accumulation of ROS (36). Based on these observations, we can develop a model for the negative regulation of ROS levels by SA (*SI Appendix*, Fig. S8*C*). According to this model, SA levels were increased in the mutants containing the *anac090* mutation, which activates an antioxidant defense system by increasing the levels of SA-inducible redoxins (e.g., GRXC9 in *SI Appendix*, Fig. S8*B*) and glutathione, in turn leading to a reduction in ROS levels (*SI Appendix*, Fig. S8*C*). In *anac017/090* mutants, ROS levels are expected to increase due to the loss of ANAC017 but also to decrease due to the loss of ANAC090 and increased SA. This opposing regulation of ROS levels might explain why ROS levels do not increase in the *anac017/090* mutant. This crosstalk between SA and ROS responses can maintain the levels of antioxidants sufficiently to protect the senescing leaf cells from premature death, ensuring the slow degeneration of cells during leaf senescence. In this regard, the SA–ROS crosstalk at the early stage of leaf senescence might be critical to prevent an oxidative burst and acute cell death in response to environmental stresses.

A number of studies have previously reported the associations of the NAC TF family with ROS and SA responses. First, increased ROS levels, owing to a decline in antioxidant capacity, are highly associated with the progression of leaf senescence (36). $H_2O_2$ treatment was reported to induce the expression of several senescence-associated *NAC*s, such as *ANAC029/AtNAP*, *ANAC002/ATAF1*, *ANAC042/JUB1*, and *ANAC059/ORS1* (20, 23, 37). Among them, ANAC042 was reported as the only negative regulator of leaf senescence that modulates cellular $H_2O_2$ levels (23). Interestingly, however, *ANAC017* is not induced by $H_2O_2$, although it mediates $H_2O_2$ responses in plants (32) and, according to our data, loss of ANAC017 triggers increased ROS levels (Fig. 4*D*) and accelerates leaf senescence (Fig. 2). These data suggest that ANAC017, compared with the other ROS-induced NACs, acts as an upstream master negative regulator of ROS response with no feedback regulatory loop from ROS on its expression. Second, SA levels were previously shown to be low in young leaves but high in senescing leaves (38, 39), and overexpression of the *S3H* gene encoding an SA 3-hydroxylase reduced SA levels and delayed leaf senescence (40), suggesting that SA contributes to the promotion of leaf senescence. However, little is known about NACs that regulate SA-mediated leaf senescence. *CBNAC/NTL9* and *ANAC081/ATAF2* were increased in their expression levels after exposure to SA (41, 42), but they played no significant roles in leaf senescence according to our data (*SI Appendix*, Fig. S8*D*), suggesting that they contribute to SA-mediated pathogen resistance (41, 43) rather than to SA-mediated leaf senescence. In this study, we identified ANAC090 as a negative regulator of SA-mediated leaf senescence; loss of ANAC090 led to increased SA levels (Fig. 4*C*) and accelerated leaf senescence (Fig. 2). Of note, previous genetic studies have not identified ANAC090 in association with leaf senescence. Senescence-associated NACs have been identified mostly based on the alteration in their expression levels during leaf senescence. However, *ANAC090* is not induced by SA treatment, and its expression drops to the basal level at the late-senescence stage, unlike known senescence-associated *NAC*s (*SI Appendix*, Fig. S8*A*). Also, dysfunction of ANAC090 causes no severe alteration in morphological phenotype during leaf senescence. These data demonstrate the unique value of our time-evolving network-based approach for identifying senescence regulators such as ANAC090. Furthermore, our approach can be applied to other TF families, such as the WRKY and MYB families, to identify key presenescence regulators in these TF families.

## Materials and Methods

**Plant Materials and Growth Conditions.** *Arabidopsis thaliana* ecotype Columbia (Col) was the parent strain for all mutants used in this study. The transfer DNA (T-DNA) insertion lines of *NAC* genes were obtained from the SALK T-DNA insertion collection, SAIL collection, or GABI-KAT collection (44–46). The genotype of each single- or double-mutant line was confirmed by PCR-based genotyping (*SI Appendix*, Table S1). For the *ANAC017-HA*, *ANAC082-HA*, and *ANAC090-HA* or *ANAC090-GFP* overexpression lines, cDNAs covering the complete coding sequence were cloned into *pCR-CCD_F* (47) and were recombined into the gateway version of the *pCsVMV-HA3-N-1300* or *pCsVMV-GFP-N-1300* vector. Plants used for most experiments were grown in an environmentally controlled growth room under a 16-h/8-h light/dark cycle (photon flux density 100 $\mu mol \cdot m^{-2} \cdot s^{-1}$) at 22 °C.

**Data Availability.** The raw and normalized data of the NanoString nCounter assay and RNA-sequencing have been deposited in the National Center for Biotechnology Gene Expression Omnibus database (48) with the accession numbers of GSE92369 and GSE92314, respectively, under the GEO SuperSeries accession no. GSE92371.

More detailed information regarding the experimental and computational procedures used in this study is provided in *SI Appendix, SI Materials and Methods*.

**ACKNOWLEDGMENTS.** We thank Wonhee Lee and Sukjoon Jung for insightful discussions. This research was supported by Institute for Basic Science Grants IBS-R013-D1 (to H.J.K., J.G.K., J.J.K., S.H., J.K., J.H.K., and H.G.N.) and IBS-R013-A1 (to J.-H.P. and D.H.) and by the Mid-career Researcher Program through National Research Foundation of Korea (funded by the Ministry of Science, ICT and Future Planning) Grants 2015R1A2A2A01005820 (to H.R.W.) and 2017R1A2B4012937 (to P.O.L.).

1. Lim PO, Kim HJ, Nam HG (2007) Leaf senescence. *Annu Rev Plant Biol* 58:115–136.
2. Oh SA, et al. (1997) Identification of three genetic loci controlling leaf senescence in Arabidopsis thaliana. *Plant J* 12:527–535.
3. Woo HR, Kim HJ, Nam HG, Lim PO (2013) Plant leaf senescence and death–Regulation by multiple layers of control and implications for aging in general. *J Cell Sci* 126: 4823–4833.
4. Kim HJ, Nam HG, Lim PO (2016) Regulatory network of NAC transcription factors in leaf senescence. *Curr Opin Plant Biol* 33:48–56.
5. Woo HR, et al. (2016) Programming of plant leaf senescence with temporal and inter-organellar coordination of transcriptome in Arabidopsis. *Plant Physiol* 171:452–467.
6. Breeze E, et al. (2011) High-resolution temporal profiling of transcripts during Arabidopsis leaf senescence reveals a distinct chronology of processes and regulation. *Plant Cell* 23:873–894.
7. Penfold CA, Buchanan-Wollaston V (2014) Modelling transcriptional networks in leaf senescence. *J Exp Bot* 65:3859–3873.
8. Allu AD, Soja AM, Wu A, Szymanski J, Balazadeh S (2014) Salt stress and senescence: Identification of cross-talk regulatory components. *J Exp Bot* 65:3993–4008.
9. Jaradat MR, Feurtado JA, Huang D, Lu Y, Cutler AJ (2013) Multiple roles of the transcription factor AtMYBR1/AtMYB44 in ABA signaling, stress responses, and leaf senescence. *BMC Plant Biol* 13:192.

10. Zhang X, et al. (2011) The R-R-type MYB-like transcription factor, AtMYBL, is involved in promoting leaf senescence and modulates an abiotic stress response in Arabidopsis. *Plant Cell Physiol* 52:138–148.
11. Besseau S, Li J, Palva ET (2012) WRKY54 and WRKY70 co-operate as negative regulators of leaf senescence in Arabidopsis thaliana. *J Exp Bot* 63:2667–2679.
12. Zentgraf U, Laun T, Miao Y (2010) The complex regulation of WRKY53 during leaf senescence of Arabidopsis thaliana. *Eur J Cell Biol* 89:133–137.
13. Robatzek S, Somssich IE (2001) A new member of the Arabidopsis WRKY transcription factor family, AtWRKY6, is associated with both senescence- and defence-related processes. *Plant J* 28:123–133.
14. Zhou X, Jiang Y, Yu D (2011) WRKY22 transcription factor mediates dark-induced leaf senescence in Arabidopsis. *Mol Cells* 31:303–313.
15. Guo Y, Gan S (2011) AtMYB2 regulates whole plant senescence by inhibiting cytokinin-mediated branching at late stages of development in Arabidopsis. *Plant Physiol* 156:1612–1619.
16. Huang CK, et al. (2015) A single-repeat MYB transcription repressor, MYBH, participates in regulation of leaf senescence in Arabidopsis. *Plant Mol Biol* 88:269–286.
17. Jensen MK, et al. (2010) The Arabidopsis thaliana NAC transcription factor family: Structure-function relationships and determinants of ANAC019 stress signalling. *Biochem J* 426:183–196.
18. Podzimska-Sroka D, O'Shea C, Gregersen PL, Skriver K (2015) NAC transcription factors in senescence: From molecular structure to function in crops. *Plants (Basel)* 4: 412–448.
19. Kim JH, et al. (2009) Trifurcate feed-forward regulation of age-dependent cell death involving miR164 in Arabidopsis. *Science* 323:1053–1057.
20. Balazadeh S, et al. (2011) ORS1, an $H_2O_2$-responsive NAC transcription factor, controls senescence in Arabidopsis thaliana. *Mol Plant* 4:346–360.
21. Kim YS, Sakuraba Y, Han SH, Yoo SC, Paek NC (2013) Mutation of the Arabidopsis NAC016 transcription factor delays leaf senescence. *Plant Cell Physiol* 54:1660–1672.
22. Guo Y, Gan S (2006) AtNAP, a NAC family transcription factor, has an important role in leaf senescence. *Plant J* 46:601–612.
23. Wu A, et al. (2012) JUNGBRUNNEN1, a reactive oxygen species-responsive NAC transcription factor, regulates longevity in Arabidopsis. *Plant Cell* 24:482–506.
24. Yang SD, Seo PJ, Yoon HK, Park CM (2011) The Arabidopsis NAC transcription factor VNI2 integrates abscisic acid signals into leaf senescence via the COR/RD genes. *Plant Cell* 23:2155–2168.
25. Kim HJ, et al. (2014) Gene regulatory cascade of senescence-associated NAC transcription factors activated by ETHYLENE-INSENSITIVE2-mediated leaf senescence signalling in Arabidopsis. *J Exp Bot* 65:4023–4036.
26. Jin J, et al. (2017) PlantTFDB 4.0: Toward a central hub for transcription factors and regulatory interactions in plants. *Nucleic Acids Res* 45:D1040–D1045.
27. Woo HR, et al. (2010) The RAV1 transcription factor positively regulates leaf senescence in Arabidopsis. *J Exp Bot* 61:3947–3957.
28. Geiss GK, et al. (2008) Direct multiplexed measurement of gene expression with color-coded probe pairs. *Nat Biotechnol* 26:317–325.
29. Barabási AL, Oltvai ZN (2004) Network biology: Understanding the cell's functional organization. *Nat Rev Genet* 5:101–113.
30. Lee HJ, et al. (2010) Direct transfer of alpha-synuclein from neuron to astroglia causes inflammatory responses in synucleinopathies. *J Biol Chem* 285:9262–9272.
31. Huang W, Sherman BT, Lempicki RA (2009) Systematic and integrative analysis of large gene lists using DAVID bioinformatics resources. *Nat Protoc* 4:44–57.
32. Ng S, et al. (2013) A membrane-bound NAC transcription factor, ANAC017, mediates mitochondrial retrograde signaling in Arabidopsis. *Plant Cell* 25:3450–3471.
33. Gadjev I, et al. (2006) Transcriptomic footprints disclose specificity of reactive oxygen species signaling in Arabidopsis. *Plant Physiol* 141:436–445.
34. Ernst HA, Olsen AN, Larsen S, Lo Leggio L (2004) Structure of the conserved domain of ANAC, a member of the NAC family of transcription factors. *EMBO Rep* 5:297–303.
35. Olsen ANEH, Lo Leggio L, Skriver K (2005) DNA-binding specificity and molecular functions of NAC transcription factors. *Plant Sci* 169:785–797.
36. Rogers H, Munné-Bosch S (2016) Production and scavenging of reactive oxygen species and redox signaling during leaf and flower senescence: Similar but different. *Plant Physiol* 171:1560–1568.
37. Balazadeh S, Wu A, Mueller-Roeber B (2010) Salt-triggered expression of the ANAC092-dependent senescence regulon in Arabidopsis thaliana. *Plant Signal Behav* 5:733–735.
38. Morris K, et al. (2000) Salicylic acid has a role in regulating gene expression during leaf senescence. *Plant J* 23:677–685.
39. Khan M, Rozhon W, Poppenberger B (2014) The role of hormones in the aging of plants–A mini-review. *Gerontology* 60:49–55.
40. Zhang K, Halitschke R, Yin C, Liu CJ, Gan SS (2013) Salicylic acid 3-hydroxylase regulates Arabidopsis leaf longevity by mediating salicylic acid catabolism. *Proc Natl Acad Sci USA* 110:14807–14812.
41. Kim HS, et al. (2012) A NAC transcription factor and SNI1 cooperatively suppress basal pathogen resistance in Arabidopsis thaliana. *Nucleic Acids Res* 40:9182–9192.
42. Delessert C, et al. (2005) The transcription factor ATAF2 represses the expression of pathogenesis-related genes in Arabidopsis. *Plant J* 43:745–757.
43. Alves MS, et al. (2014) Transcription factor functional protein-protein interactions in plant defense responses. *Proteomes* 2:85–106.
44. Kleinboelting N, Huep G, Kloetgen A, Viehoever P, Weisshaar B (2012) GABI-Kat SimpleSearch: New features of the Arabidopsis thaliana T-DNA mutant database. *Nucleic Acids Res* 40:D1211–D1215.
45. Alonso JM, Stepanova AN (2003) T-DNA mutagenesis in Arabidopsis. *Methods Mol Biol* 236:177–188.
46. Sessions A, et al. (2002) A high-throughput Arabidopsis reverse genetics system. *Plant Cell* 14:2985–2994.
47. Kim J, Somers DE (2010) Rapid assessment of gene function in the circadian clock using artificial microRNA in Arabidopsis mesophyll protoplasts. *Plant Physiol* 154: 611–621.
48. Edgar R, Domrachev M, Lash AE (2002) Gene expression omnibus: NCBI gene expression and hybridization array data repository. *Nucleic Acids Res* 30:207–210.